The Stability of Short Symmetric Internal Waves on Sloping Fronts: Beyond the Traditional Approximation

ALAIN COLIN DE VERDIÈRE

Laboratoire de Physique des Oceans, Universite de Bretagne Occidentale, Brest, France

(Manuscript received 17 March 2011, in final form 12 October 2011)

ABSTRACT

The interaction of internal waves with geostrophic flows is found to be strongly dependent upon the background stratification. Under the traditional approximation of neglecting the horizontal component of the earth's rotation vector, the well-known inertial and symmetric instabilities highlight the asymmetry between positive and negative vertical components of relative vorticity (horizontal shear) of the mean flow, the former being stable. This is a strong stratification limit but, if it becomes too low, the traditional approximation cannot be made and the Coriolis terms caused by the earth's rotation vector must be kept in full. A new asymmetry then appears between positive and negative horizontal components of relative vorticity (vertical shear) of the mean flow, the latter becoming more unstable. Particularly conspicuous at low latitudes, this new asymmetry does not require vanishing stratification to occur as it operates readily for rotation/stratification ratios $2\Omega/N$ as small as 0.25 (the stratification still dominates over rotation) for realistic vertical shears. Given that such ratios are easily found in ocean–atmosphere boundary layers or in the deep ocean, such ageostrophic instabilities may be important for the routes to dissipation of the energy of the large-scale motions. The energetics show that, depending on the orientation of the internal wave crests with respect to the mean isopycnal surfaces, the unstable motions can draw their energy either from the kinetic energy or from the available potential energy of the mean flow. The kinetic energy source is usually the leading contribution when the growth rates reach their maxima.

1. Introduction

Internal waves are often analyzed as perturbations of a stably stratified fluid at rest. Ocean and atmosphere are indeed stratified but not at rest. When such situations occur, instability theory takes over to find out whether imposed mean flows are stable or unstable to infinitesimal or finite amplitude perturbations. At sufficiently large scales the basic state is geostrophic with vertical shear equilibrated by the slope of the density surfaces. For vigorous oceanic mesoscale eddies or jets, observations show vertical variations of isopycnal surfaces on the order of 500 m over, for example, 50 km or a slope of 1%. Because the slope is so small, the interaction of internal waves with mean flows is often studied in the context of a flat horizontal background stratification. For waves with frequencies in the range of the Brunt–Väisälä frequency, particle displacements are nearly vertical, making this approximation an excellent one. At low enough frequency, rotation becomes important and the choice of a flat horizontal stratification becomes questionable.

The interaction of a mean vertical shear with internal gravity waves has a long history [for a review, see Drazin and Reid (1981)]. In the three-dimensional case, the wave–mean flow interaction is governed by what happens at critical layers (Booker and Bretherton 1967; Lindzen 1988). With the addition of rotation, the mean vertical shear is in thermal wind balance and a sloping stratification occurs. The modification of the critical layer conditions caused by rotation was studied by Jones (1967) on the f plane and Grimshaw (1975) in the general case. The effect of a sloping stratification on the propagation of stable internal waves was considered by Mooers (1975) on the f plane.

More generally, the specific instabilities of waves on sloping density surfaces fall into two categories. First, for motions of subinertial frequencies, that is, frequencies much lower than the inertial frequency f, three-dimensional, quasigeostrophic waves are found to become unstable

Corresponding author address: Alain Colin de Verdière, Université de Bretagne Occidentale, Laboratoire de Physique des Océans, 6 Ave Le Gorgeu, C.S. 93837, 29238 Brest CEDEX 3, France.
E-mail: acolindv@univ-brest.fr

DOI: 10.1175/JPO-D-11-067.1

when the gradient of potential vorticity changes sign, the source of energy comes from the available mean potential energy associated with the sloping isopycnals and the most unstable waves have scales of the order of the Rossby radius of deformation. The theories formulated by Charney (1947) and Eady (1949) have been hugely successful to rationalize the eddy energy containing scale in both the atmosphere and ocean. The second category is symmetric instability (also called slantwise convection), which operates in an ageostrophic regime and supposes that the perturbations are two dimensional (uniform along the direction of the mean flow). They were shown by Stone (1966) to compete in terms of growth rates with the quasigeostrophic instabilities for low enough Richardson numbers. Hoskins (1974) showed them to be a variant of the inertial instability found by Rayleigh (1917), the necessary condition for instability amounting to the vanishing of Ertel potential vorticity. The initial context of application was the atmosphere and the circumpolar vortex (Ooyama 1966; Charney 1973)—hence the name symmetric for those perturbations independent of longitude. Whether and how such symmetric waves became unstable was studied by many authors (Ooyama 1966; Bennett and Hoskins 1979; Xu and Clark 1985; Sun 1995). Application of the theory has shifted from the large-scale circumpolar vortex to the formation of rainbands in mesoscale fronts (Bennett and Hoskins 1979; Seltzer et al. 1985; and reviews by Emmanuel 1994; Bluestein 1993). Symmetric instability in the ocean is starting to be considered an important process during episodes of convective deep-water formation (Haine and Marshall 1998) and in the surface mixed layer in the presence of horizontal temperature gradients (Taylor and Ferrari 2010). It has been recently invoked by Joyce et al. (2009) to rationalize some of the mixing events observed in the vicinity of the Gulf Stream front. The interaction of internal gravity waves with geostrophic mean flows is important to study in the large-scale context of the ocean circulation because internal waves are suspected to be the missing link to account for the required diapycnal transport and energy dissipation of the circulation (Wunsch and Ferrari 2004).

There has been a renewed interest in recent years about the dynamical consequences of a finite angle between the gravity and the rotation vector abandoning hydrostatics and the so-called traditional approximation, which neglects the horizontal component of the earth's rotation. Convection experiments in the laboratory by Sheremet (2004) and in idealized numerical experiments by Straneo et al. (2002) and Wirth and Barnier (2008) point out that convective plumes tend to be organized along the direction of the rotation axis (and not gravity) even far into the turbulent regime. Symmetric instability without making the traditional approximation was addressed by Sun (1995), who found that it introduced an asymmetry between positive and negative values of vertical shears of the mean flow. The usually neglected nontraditional Coriolis terms were added recently in Stone's instability problem by Jeffery and Wingate (2009), who found that it increased the dominance of symmetric over baroclinic instabilities in regions of weak stratification, such as the Labrador Sea.

From the above succinct review, it appears that a unified treatment of the interaction of internal gravity waves with vertical and horizontal shear of the mean flow, full representation of the earth's rotation vector, and arbitrary stratification is still missing. The objective of this paper is to provide such a unified view in the hope to find out if some important new process may emerge for a particular combination of the above factors. The previous authors all point out that a correct representation of the earth's rotation vector becomes crucial when the stratification is weak, and it is precisely in this region of parameter space that some new results will emerge. Even for linearized problems such a broad scope requires simplifications. First, the waves are allowed to vary only in the plane normal to the mean flow thereby filtering out critical layer instabilities, hence the term symmetric in the title of this paper. Furthermore only short internal gravity waves are considered so that the vertical and horizontal shears and stratification of the background state are taken as constant.

Given these assumptions, this paper provides answers to the following questions:

(i) With the exception of Sun (1995), it is usually assumed that the meridional component of the earth's rotation is negligible for the internal wave–geostrophic mean flow interaction problem. Does it become important if at all? Do certain latitudes favor the interaction?
(ii) In symmetric instability, it is often assumed a priori that the motions lie along mean isopycnal surfaces. In such a case the energy source can only be the kinetic energy of the mean flow through the action of Reynolds's stresses. However, is this always true and under which conditions does the available potential energy associated with the sloping background stratification come into play?

Section 2 provides the central, horizontal vorticity equation that governs the dynamics of internal gravity waves on a mean zonal flow. The marginal stability conditions are found analytically in section 3. It includes the full dependencies on stratification, latitude, and horizontal and vertical shears. The question of the energy sources is discussed in section 4. Section 5 presents maps of the growth rates in the unstable case and points out the fundamental importance of the meridional component of the earth's rotation when the stratification is low enough. This is concluded by a general discussion in section 6.

2. The governing equations

We consider the dynamics of perturbations of a mean flow in thermal wind equilibrium, with stable stratification (Brunt–Väisälä frequency $N^2 > 0$). There is no difficulty and definite conceptual advantage in keeping the full Coriolis forces, so the traditional approximation of neglecting the meridional component of the earth's rotation is not made, suppressing the restriction to shallow water motions. Because the interest is focused on the high frequency waves, the causes for the existence of baroclinic quasigeostrophic waves are suppressed by neglecting mean potential vorticity gradients (beta effect, varying topography, and undulation of the isopycnal surfaces) and leaving aside boundary effects. This constant potential vorticity case is meaningful only if the scales of the waves are assumed to be smaller than any lateral inhomogeneities due to rotation, stratification, topography, or mean flows. Filtering inflection-point-type instabilities requires a short wavelength approximation; that is, the mean flow will vary only linearly (horizontally and/or vertically).

The analysis is given here for zonal mean flows with mean isopycnals sloping in the meridional direction. The x, y, and z axes are in the eastward, northward, and upward vertical directions, respectively, and the equations governing the mean flow velocity $[U(y, z), 0, 0]$ are then

$$fU = -\frac{1}{\rho_0}\frac{\partial P}{\partial y} \tag{1a}$$

and

$$-\tilde{f}U = -\frac{1}{\rho_0}\frac{\partial P}{\partial z} + B, \tag{1b}$$

implying the generalized thermal wind equation,

$$(2\Omega \cdot \nabla)U = -\frac{\partial B}{\partial y} \tag{1c}$$

in which $f = 2\Omega \sin\phi$, $\tilde{f} = 2\Omega\cos\phi$ (ϕ is latitude), and $2\Omega = (0, \tilde{f}, f)$ in (1c) is twice the earth's rotation vector. The quantity B is the mean buoyancy $(= -g\rho/\rho_0)$, so $\partial B/\partial z$ is the mean Brunt–Väisälä frequency N^2. Since the mean flow lies along B contours, the buoyancy conservation equation is also satisfied. Note that Eqs. (1a)–(1c) are exact in the sense that horizontal or vertical shears of the zonal flow are arbitrary: (1a)–(1c) are not a small Rossby number approximation of the Euler equations. The generalized thermal wind equation (1c) has been proposed in a discussion of the equatorial context by Colin de Verdière and Schopp (1994). Because of its importance for the ocean, only zonal mean flows are considered here, but note that this case favors the role of the nontraditional Coriolis terms.

The analysis is restricted to symmetric wave perturbations with no x variation along the mean flow direction. The linear perturbations in terms of $\mathbf{u} = (u, v, w)$, p and b obey the following equations:

$$\frac{\partial u}{\partial t} + v\frac{\partial U}{\partial y} + w\frac{\partial U}{\partial z} - fv + \tilde{f}w = 0, \tag{2a}$$

$$\frac{\partial v}{\partial t} + fu = -\frac{1}{\rho_0}\frac{\partial p}{\partial y}, \tag{2b}$$

$$\frac{\partial w}{\partial t} - \tilde{f}u = -\frac{1}{\rho_0}\frac{\partial p}{\partial z} + b, \tag{2c}$$

$$\frac{\partial b}{\partial t} + v\frac{\partial B}{\partial y} + w\frac{\partial B}{\partial z} = 0, \tag{2d}$$

$$\frac{\partial v}{\partial y} + \frac{\partial w}{\partial z} = 0. \tag{2e}$$

The terms at the origin of the present work are the $\tilde{f}$ Coriolis terms, the shear terms in (2a), and the advection through the lateral buoyancy gradient in (2d). This last term is usually considered insignificant for internal waves but, as argued previously, this is an impossible assumption to defend for quasi-horizontal waves. Because of (2e), a streamfunction can be introduced for the perturbations velocities v and w,

$$v = -\frac{\partial \Psi}{\partial z} \quad w = \frac{\partial \Psi}{\partial y}.$$

The equation for the x component of vorticity can be obtained by cross differentiation of (2b) and (2c),

$$\frac{\partial \varsigma_x}{\partial t} = (2\Omega \cdot \nabla)u + \frac{\partial b}{\partial y}. \tag{3}$$

The zonal vorticity component ς_x can change through tilting of the earth's vorticity by the shear of the perturbations and by buoyancy torques. Time derivation of (3) and elimination of u and b with the help of (2a) and (2d) and use of (1c) provides the equation:

$$\frac{\partial^2 \varsigma_x}{\partial t^2} + 2\Omega \cdot \nabla(\mathbf{Z_a} \times \mathbf{u} \cdot \mathbf{i}) - \frac{\partial v}{\partial y}(2\Omega \cdot \nabla U) + \frac{\partial w}{\partial y}\frac{\partial B}{\partial z} = 0, \tag{4}$$

where

$$\mathbf{Z}_a = \left(0, Z_{ay} = \tilde{f} + \frac{\partial U}{\partial z}, Z_{az} = f - \frac{\partial U}{\partial y}\right)$$

is the mean absolute vorticity vector and $\mathbf{i}$ the zonal unit vector. In the following, the terms $\partial U/\partial z$ and $-\partial U/\partial y$

will be designated horizontal and vertical relative vorticity, respectively (instead of vertical and horizontal shear). After some algebra, Eq. (4) can be rewritten in terms of the sole variable Ψ:

$$\frac{\partial^2}{\partial t^2}\nabla^2\Psi + \left(\tilde{f}Z_{ay} + \frac{\partial B}{\partial z}\right)\frac{\partial^2\Psi}{\partial y^2} + fZ_{az}\frac{\partial^2\Psi}{\partial z^2} + 2fZ_{ay}\frac{\partial^2\Psi}{\partial y\partial z} = 0. \tag{5}$$

When mean flow shears are set to zero, the first three terms of (5) are readily identified with those governing the dynamics of mixed inertial–internal gravity waves with a flat background stratification (Gerkema et al. 2008). When geostrophic mean flow shears and sloping isopycnal surfaces are considered for the background state, two modifications occur in the governing equation of inertial–internal gravity waves. First, absolute vorticity appears as $\tilde{f}^2 \rightarrow \tilde{f}Z_{ay}$ in the second term and $f^2 \rightarrow fZ_{az}$ in the third. The prefactor of the fourth term (the mixed y and z derivative) $f(\tilde{f} + \partial U/\partial z)$ shows that the term exists also under the traditional approximation (provided the background state is in thermal wind balance). Its influence on the stability properties of inertial–internal gravity waves will be shown to be determinant. Equation (5) first appeared in Hua et al. (1997).

3. The dispersion relation and the marginal stability condition

Given the localness assumption, Eq. (5) is a constant coefficient partial differential equation whose solution in terms of waves can be obtained by inserting $\Psi = \mathrm{Re}[\Psi_0 e^{i(ly+mz-\omega t)}]$, yielding the dispersion relation

$$\omega^2 = \frac{(\tilde{f}Z_{ay} + \partial B/\partial z)l^2 + (fZ_{az})m^2 + 2fZ_{ay}lm}{l^2 + m^2}. \tag{6}$$

This dispersion relation has appeared in Ooyama (1966), Hoskins (1974), Mooers (1975), and Xu and Clark (1985) under the traditional f-plane approximation and in absence of vertical relative vorticity. The present version however does not make the traditional approximation of neglecting the meridional component of the earth's rotation vector. Sun (1995) has considered this same problem, but his Eq. (23) has a different factor in the last term of (6) whose origin is connected to a lack of consistency in the dynamics because that author makes the traditional approximation for the background state but not for the waves. Introducing the angle θ between the wavenumber vector and the y axis allows (6) to be rewritten as

$$\omega^2 = \left(\tilde{f}Z_{ay} + \frac{\partial B}{\partial z}\right)\cos^2\theta + fZ_{az}\sin^2\theta + fZ_{ay}\sin2\theta. \tag{7}$$

As for classical inertial or internal gravity waves, the frequency depends only on the orientation of the wavenumber vector so that the waves are fully anisotropic. In the absence of shear, the frequencies are bounded (Gerkema et al. 2008), but no such conclusion can be reached when a mean flow is present because each of the coefficients in (7) may become negative for sufficiently strong shear. The dispersion relation can be rewritten nondimensionally with $\omega' = \omega/2\Omega$:

$$\begin{aligned}\omega'^2 &= \cos^2\phi(1 + \mu^{-2} + \mu^{-1}\mathrm{Ri}^{-1/2})\cos^2\theta \\ &\quad + \sin^2\phi(1 + \mathrm{Ro}_z)\sin^2\theta \\ &\quad + \cos\phi\sin\phi(1 + \mu^{-1}\mathrm{Ri}^{-1/2})\sin2\theta.\end{aligned} \tag{8}$$

Three well-known adimensional numbers are introduced in (8), namely the Richardson number $\mathrm{Ri} = N^2/(\partial U/\partial z)^2$ and the Rossby number $\mathrm{Ro}_z = (-\partial U/\partial y)/(2\Omega\sin\phi)$, which measure the vertical relative vorticity against that of the earth and a latitude-dependent parameter $\mu = 2\Omega\cos\phi/N$, which measures rotation against stratification. Note that the term involving $\mathrm{Ri}^{1/2}$ in (8) is defined to be positive or negative according to the sign of $\partial U/\partial z$. The expression (8) is put under the form

$$\omega'^2 = b\cos^2\theta + a\sin^2\theta + d\sin2\theta. \tag{9}$$

By writing ½$(b - a) = r\cos\lambda$ and $d = r\sin\lambda$, (9) can be rewritten as

$$\omega'^2 = r\cos(2\theta - \lambda) + \frac{1}{2}(b + a). \tag{10}$$

If $a + b > 0$, the frequency range of the waves is simply $[-r + ½(b + a); +r + ½(b + a)]$. When the lower bound $-r + ½(b + a) > 0$, the solutions of (5) are periodic waves modified by the presence of the shear of the mean flow. If the lower bound vanishes, the waves are neutral to become unstable when it becomes negative.

If $a + b < 0$, there is at least one value of θ $(=\lambda/2 + \pi/4)$ for which the rhs of (10) is negative; therefore, the flow is always unstable.

Note that $\mathrm{Re}(\omega')$ is zero at the marginal state, a result shown by Hua et al. (1997) to derive from the self-adjoint property of the spatial operator in (5). There is therefore an exchange of stability from periodic waves to a nonoscillatory flow. From the definition of r, it is not difficult to show that the steady marginal flow occurs for the two conditions, $ab = d^2$ and $a + b = 0$. After some algebra, the condition $ab = d^2$ becomes

$$\mathrm{Ro}_z[\mu\mathrm{Ri}^{1/2} + (1 + \mu^2)\mathrm{Ri}] + (\mathrm{Ri} - 1 - \mu\mathrm{Ri}^{1/2}) = 0. \tag{11}$$

Note that the reference to latitude now appears only through Ro_z and μ. The parameter μ summarizes the influence of the meridional component of the earth's rotation vector, whose role will therefore be maximized at low latitudes and low stratification. Background Brunt–Väisälä frequencies for the lower atmosphere or ocean lead to values of μ $O(10^{-2})$ or $O(10^{-1})$, respectively; that is, stratification dominates rotation, which indeed gives credit to the traditional approximation. Of course, this cannot be true in regions where convective or mechanical mixing has eroded the stratification. Finding out the effects of a varying stratification in (11) is not convenient because both Ri and μ vary with N and it is better to use

$$\mathrm{Ro}_y = \frac{\partial U/\partial z}{2\Omega \cos\phi}$$

instead of Ri. This second Rossby number Ro_y measures the horizontal (meridional) relative vorticity against that of the earth. The bulk of the kinetic energy of observed flows in the ocean is associated with balanced flows for which the vertical Rossby number Ro_z is smaller than one. By contrast, observed vertical shears show that this horizontal Rossby number Ro_y can be much larger than one. It can be expressed readily in terms of Ri and μ as $\mathrm{Ro}_y = \mu^{-1}\mathrm{Ri}^{-1/2}$ so that (11) becomes

$$\mathrm{Ro}_z(\mu^{-2} + \mathrm{Ro}_y + 1) + [\mu^{-2} - \mathrm{Ro}_y^2 - \mathrm{Ro}_y] = 0. \tag{12}$$

The complicated relations (11) or (12) have a rather simple origin. Let us complete (3) and write the governing equations for the y and z vorticity components as

$$\frac{\partial \varsigma_y}{\partial t} = (\mathbf{Z_a} \cdot \nabla)v, \quad \frac{\partial \varsigma_z}{\partial t} = (\mathbf{Z_a} \cdot \nabla)w. \tag{13}$$

Since the vortex stretching terms vanish for the marginal state, the velocity must be constant in the direction of the absolute vorticity vector $\mathbf{Z}_a$. Furthermore, the buoyancy equation (2d) requires the velocity vector to lie along mean isopycnal surfaces in steady flow. Then, from continuity the velocity can vary only in the direction normal to these surfaces. For a nontrivial flow to be possible, the absolute vorticity vector must also lie along the isopycnal surfaces:

$$\mathbf{Z}_a \cdot \nabla B = 0. \tag{14}$$

However, $\mathbf{Z}_a \cdot \nabla B$ is the Ertel potential vorticity of the mean state, which has to be zero for a neutral perturbation to exist. From the previous expression of $\mathbf{Z}_a$ and use of (1c), it can be shown that the zero potential vorticity (PV) condition (14) leads precisely to (11) or (12). The marginality condition (11) involves the three independent parameters Ri, Ro_z, and μ [or the combination Ro_y, Ro_z, μ in (12)], making the conditions of instability rather difficult to extract. The analysis that is performed next allows one to explore the sensitivities to stratification, rotation, mean shears, and latitude.

a. Strong stratification: $\mu \ll 1$

If $\mu = 0$, the effect of the horizontal component of the earth's rotation disappears altogether and (11) simplifies to

$$\mathrm{Ro}_z = (-1 + \mathrm{Ri}^{-1})$$

or

$$\mathrm{Ri} = \frac{1}{\mathrm{Ro}_z + 1}, \tag{15}$$

which is the marginal symmetric instability condition discussed by Bluestein (1993) and Emmanuel (1994). Note that the condition involves only the square of vertical shear through Ri, and the instability is therefore independent of its sign. In this limit of strong stratification, the marginality condition (15) reduces to $\mathrm{Ri} \approx 1$ for balanced, quasigeostrophic flows ($\mathrm{Ro}_z \ll 1$), the well-known condition for symmetric instability (Stone 1966). By using (1c), this condition can also be expressed as a condition on the mean isopycnal slope s:

$$s = -\frac{\partial B/\partial y}{\partial B/\partial z} \approx f/N\mathrm{Ri}^{-1/2} \tag{16}$$

so that the marginality condition $\mathrm{Ri} \approx 1$ also means that the critical slope $|s|$ is equal to $|f|/N$ or equivalently that the Burger number $(f^{-1}Ns)^2$ is unity. In the Rossby adjustment problem the radiation of inertial gravity waves is called for to explain how the scales of quasigeostrophic motions adjust to the internal Rossby radius of deformation. Here, by contrast, the same $O(1)$ Burger number end state is found for reasons associated with the marginal stability of the internal gravity waves themselves.

When horizontal and vertical relative vorticity are present, the instability depends very much on the sign of vertical relative vorticity since Ri greater (less) than one is required for negative (positive) vertical relative vorticity, respectively. Hence, a mean flow with positive vertical relative vorticity is more stable than one with negative vertical relative vorticity. With such an instability operating in the ocean or atmosphere (and mean flows adapting to marginal conditions), the isopycnal slopes given by (16) are expected to be less for negative than for positive

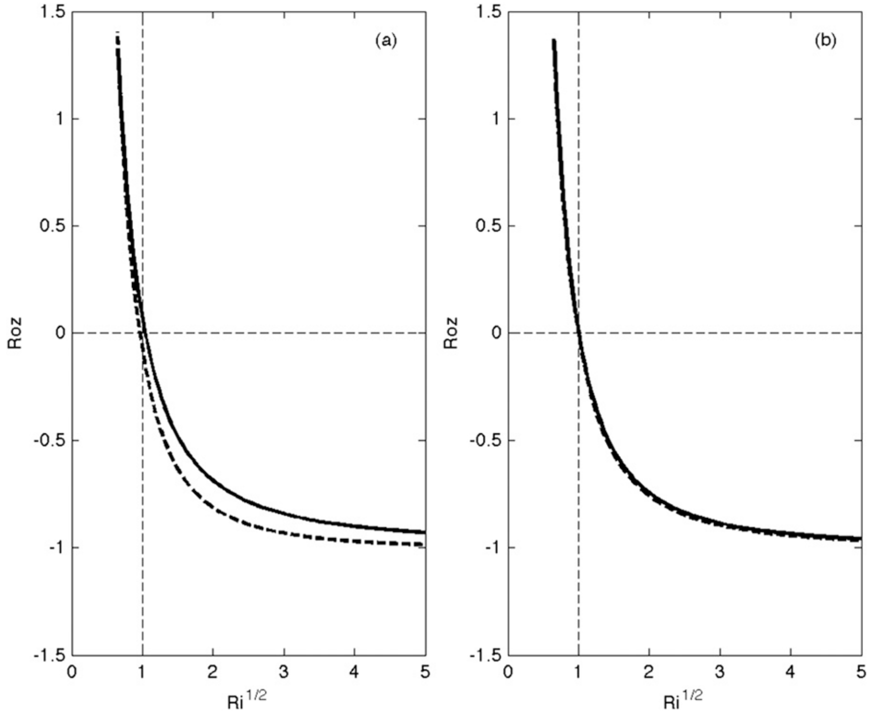

FIG. 1. The marginal curves Ro_z as a function of $|Ri^{1/2}|$ from (11) at a latitude $\phi = 45°$ for two stratifications, (a) $2\Omega/N = 0.1$ and (b) $2\Omega/N = 0.01$. Black (dashed) curves indicate positive (negative) horizontal relative vorticity. When Ri is very large, the instability occurs as inertial instability ($Ro_z < -1$). As Ri decreases, the horizontal shear required for instability decreases but still requires negative vertical relative vorticity ($Ro_z < 0$). As $Ri < 1$, flows with positive vertical relative vorticity ($Ro_z > 0$) become unstable as well. Although stratification dominates rotation in these examples, an asymmetry between positive and negative horizontal relative vorticity is already apparent in (a).

relative vorticity and the same will be true of the associated flows from (1c).

In cases of vanishing horizontal relative vorticity or very large stratification ($Ri \rightarrow \infty$), the marginality condition (15) becomes simply $Ro_z \rightarrow -1$, the inertial Rayleigh instability limit for horizontal flows for which the vertical absolute vorticity Z_{az} vanishes. Introduced for homogeneous fluids, inertial instability is recovered in the strong stratification limit. The vertical velocities become very small and the second term of the dispersion relation (7) then dominates as $\theta \rightarrow \pi/2$.

The exact relation (11) is illustrated in Fig. 1 for typical atmospheric ($2\Omega/N = 0.01$) and oceanic cases ($2\Omega/N = 0.1$) at 45° latitude. For the oceanic case, a small sensitivity to the sign of vertical shear (through the sign of $Ri^{1/2}$), and hence to the meridional component of the earth's rotation, already appears.

b. From strong to weak stratification

Stratification is weak in boundary layers, in the lower atmosphere when gravitational convective instability has eroded the stratification or in the surface oceanic mixed layer. It is also weak in polar regions or the deep ocean. The relation (12) between Ro_z and Ro_y is shown in Fig. 2 for three values of $2\Omega/N = (0.01, 0.1, 1)$ at 45° latitude. The important stability differences of positive and negative vertical relative vorticity and the inertial stability limit recalled previously stand out for the smaller values of $2\Omega/N$. When $2\Omega/N$ (and therefore μ) is not so small however, the stability domain changes completely, and it becomes easier for a flow with positive vertical relative vorticity to become unstable, provided the horizontal relative vorticity (Ro_y) is large enough. Figure 3 (a zoom of Fig. 2c) reveals clearly this reduced domain of stability when $2\Omega/N = 1$. The structure of the marginal curve in Ro_z–Ro_y space can be rationalized as follows. The first term in (12) vanishes for $Ro_y = -(1 + \mu^{-2})$ so that $Ro_z \rightarrow \infty$, giving the vertical asymptote in Fig. 3. If, instead, $Ro_y \rightarrow \infty$, then $Ro_z = Ro_y - \mu^{-2}$, giving the second oblique asymptote. Note that $Ro_z = Ro_y$ means that $(2\Omega \cdot \nabla)U = 0$, which implies a flat background stratification from (1c). The first bissectrix in Fig. 3 therefore separates two regions with mean buoyancy B decreasing (increasing) poleward in

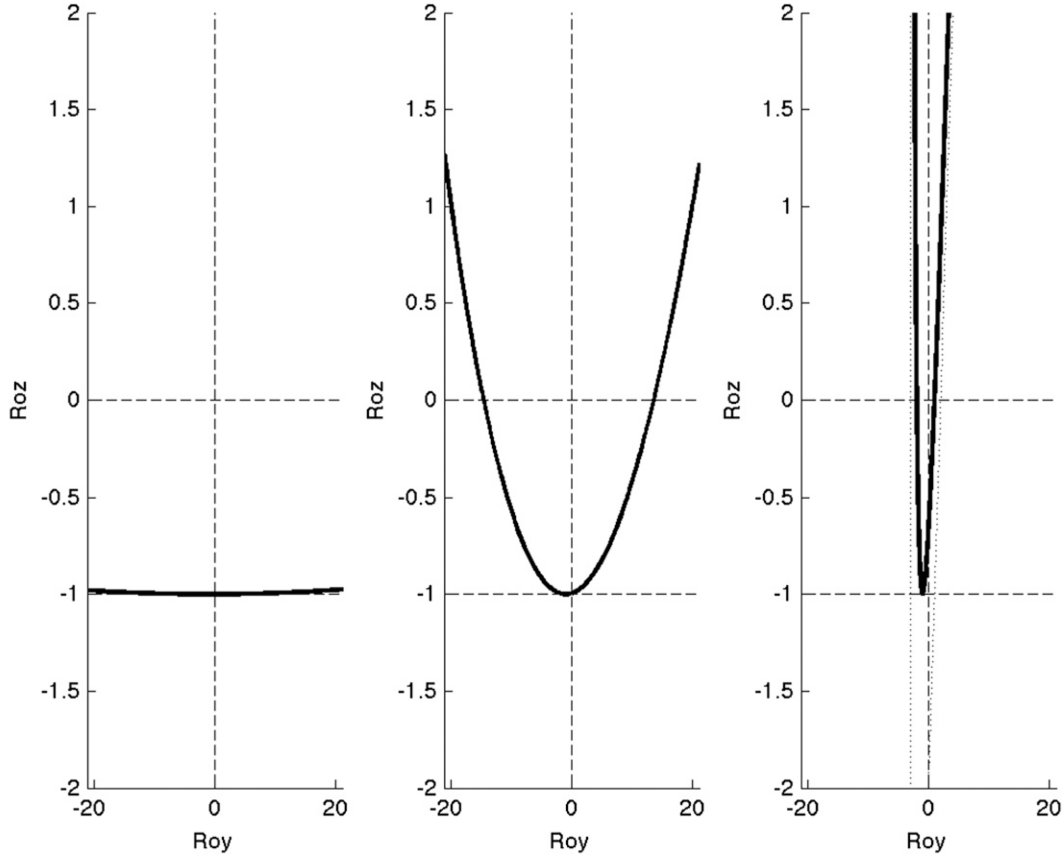

FIG. 2. The marginal curves Ro_z as a function of Ro_y at a latitude $\phi = 45°$ for (a) $2\Omega/N = 0.01$, (b) $2\Omega/N = 0.1$, and (c) $2\Omega/N = 1$. The domain of stability lies above the black curves; its reduction as the stratification decreases from (a) to (c) reveals the growing influence of the meridional component of the earth's vorticity. The dotted lines in (c) refer to the asymptotes described in the text.

the right (left) part of the figure. Further study of (12) shows the existence of two extrema. The minimum $\mathrm{Ro}_z = -1$ for $\mathrm{Ro}_y = -1$ corresponds to the condition of inertial instability when the middle term dominates in the dispersion relation (7) and the unstable motions are quasi horizontal. We have already seen in section 3b that the behavior around this local minimum dominates the dynamics for a large domain of Ro_y values when μ is small. However, there is also a maximum $\mathrm{Ro}_z = -(1 + 4\mu^{-2})$, which occurs for $\mathrm{Ro}_y = -(1 + 2\mu^{-2})$, but it can be shown to be irrelevant for the stability boundary. As shown previously, when $a + b$ is negative, the flow is always unstable, and this marginal condition written in terms of Ro_z and Ro_y is

$$\mathrm{Ro}_y + 1 + \mu^{-2} + \tan^2\phi(1 + \mathrm{Ro}_z) = 0. \quad (17)$$

The straight line (18) goes through the point of coordinates $\mathrm{Ro}_y = -(1 + \mu^{-2})$, $\mathrm{Ro}_z = -1$ and is always above the maximum, so the whole half-plane $\mathrm{Ro}_z \le -1$ is always unstable. Therefore, when $\mu = O(1)$ (stratification equals rotation), the stable region in Fig. 3 is limited by the two asymptotes: the vertical one at $\mathrm{Ro}_y = -(1 + \mu^{-2})$ and the oblique one at $\mathrm{Ro}_z = \mathrm{Ro}_y - \mu^{-2}$, and only that part of the curve (12) above the minimum $\mathrm{Ro}_y = -1$, $\mathrm{Ro}_z = -1$.

The interplay of stratification and horizontal and vertical relative vorticity on the marginal stability of zonal jets can then be summarized as follows.

1) For positive relative vertical vorticity ($\mathrm{Ro}_z > 0$), the stability domain shrinks as the stratification weakens. The flow may become unstable for sufficiently large positive or negative horizontal relative vorticity.
2) For zero relative vertical vorticity ($\mathrm{Ro}_z = 0$), the flow is stable in the interval $-1/2 - (1/4 + \mu^{-2})^{1/2} \le \mathrm{Ro}_y \le -1/2 + (1/4 + \mu^{-2})^{1/2}$. The huge stability interval for strong stratification ($\mu \ll 1$) shrinks asymptotically to the small interval $-1 \le \mathrm{Ro}_y \le 0$ for low stratification ($\mu \gg 1$).
3) For negative relative vertical vorticity ($\mathrm{Ro}_z < 0$), there remains a stability island (connected to the

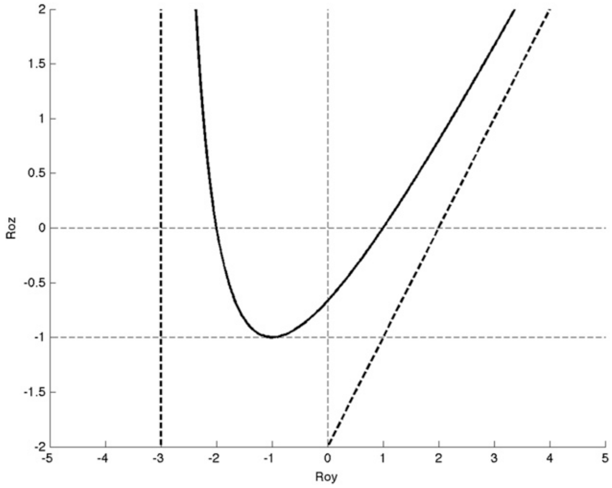

FIG. 3. The marginal curves Ro_z as a function of Ro_y (vertical shear) at a latitude $\phi = 45°$ for $2\Omega/N = 1$ (so that $\mu = 2^{-1/2}$). The flow is stable above the black curve. In this zoomed version of Fig. 2c, the vertical asymptote (bold dashed) obeys $\mathrm{Ro}_y = -(1 + \mu^{-2}) = -3$, and the oblique one (bold dashed) obeys $\mathrm{Ro}_z = \mathrm{Ro}_y - \mu^{-2} = \mathrm{Ro}_y - 2$.

above) that shrinks as μ increases. Here Ro_z must be greater than -1 (obtained for $\mathrm{Ro}_y = -1$) for the flow to be stable. Outside of this small island, the flow is unstable.

In conclusion, the reduction of the domain of stability as the stratification decreases shows clearly that the addition of the meridional component of the earth's rotation vector is favorable to the development of the instability of internal waves in zonal shear flows.

The existence of the stability boundary created by the vertical asymptote in Figs. 2c and 3 has a rather simple physical explanation because the condition $\mathrm{Ro}_y = -(1 + \mu^{-2})$ becomes, in dimensional form,

$$\tilde{f} Z_{ay} + N^2 = 0, \tag{18}$$

a condition on the y component of absolute vorticity to be equal to $-N^2/\tilde{f}$. When $N \to 0$, this is nothing but inertial Rayleigh instability but now with respect to the vanishing of the meridional component of absolute vorticity. The flow is still stratified but in the lateral (y) direction. The perturbations involve nearly vertical crests as the first term in the dispersion relation (7) dominates as $\theta \to 0$. The unstable perturbations are made of sheets of vertical motions aligned along the front. There is no preferred meridional scale to control the distributions across the front because sheets of ascending or descending motions are independent of each other since the flow is vertically nondivergent. This occurrence is possible of course only if the Coriolis forces caused by the horizontal component of the earth's rotation are kept in the dynamics. Such a parameter regime could be met in oceanic or atmospheric boundary layers when vertical stratification has first been eroded by a gravitational (convective) instability or turbulent mixing to reduce the value of N. A decrease of zonal velocity of only 0.15 m s^{-1} over a 1-km height is a mean vertical shear that is already supercritical at the equator. This interaction between zonal and vertical velocities is an inertial instability that feeds on the negative vertical shear of the mean zonal flow.

The existence of the stability boundary at the second oblique asymptote, $\mathrm{Ro}_z = \mathrm{Ro}_y - \mu^{-2}$, can be shown to be equivalent to the condition $2\boldsymbol{\Omega} \cdot \boldsymbol{\nabla} B = 0$, that is, the special case in which the earth's rotation vector $\boldsymbol{\Omega}$ is parallel to the isopycnal surfaces (which then slope upward in the poleward direction). With this condition and thermal wind (1c), the Ertel potential vorticity becomes $-f^{-1} (\partial_y B)^2$. Because it is negative, the mean flow is always unstable in such a case.

c. *From mid to low latitudes*

For the case of strong stratification ($\mu \ll 1$), the dependence on latitude of the marginal condition is captured accurately by the Rossby number Ro_z and the inverse nature of the relationship between Ro_z and Ri in (15). Reasoning from Fig. 1, suppose that the mean flow is neutral at a given latitude. Keeping constant the horizontal shear, the Rossby number $|\mathrm{Ro}_z|$ grows as f decreases. Negative (positive) vertical relative vorticity is then destabilized (stabilized) as f decreases. Hence, higher (lower) Ri [meaning less (more) horizontal relative vorticity] is then required to keep mean flows with negative (positive) vertical relative vorticity near marginality. It is difficult to assess whether this conclusion remains valid for lower stratification because of the latitudinal dependence of the three adimensional numbers in (12). Figure 4 illustrates the relation (12) recast in term of horizontal shear and vertical shear at three latitudes (45°, 10°, and 1°) for the fixed value $2\Omega/N = 0.25$. The shape of the stability domain (similar to that in Fig. 3) shows readily that, as in the previous case, flows with negative (positive) vertical relative vorticity are destabilized (stabilized) at lower latitudes. Recall that, when μ is not small, the domain of stability is structured by $\mathrm{Ro}_y \approx -(1 + \mu^{-2})$, $\mathrm{Ro}_z \approx \mathrm{Ro}_y - \mu^{-2}$, and $\mathrm{Ro}_z \geq -1$. The last condition implies that instability can occur for very small values of negative vertical relative vorticity when the latitude ϕ goes to zero (see Fig. 4). The flow can also become unstable for modest positive relative vorticity for negative Ro_y around $-(1 + \mu^{-2})$. For large positive horizontal relative vorticity, however, the situation is different. If, for instance, Ro_y is much larger than 1 and μ^{-2}, then the marginal condition (12) reduces to

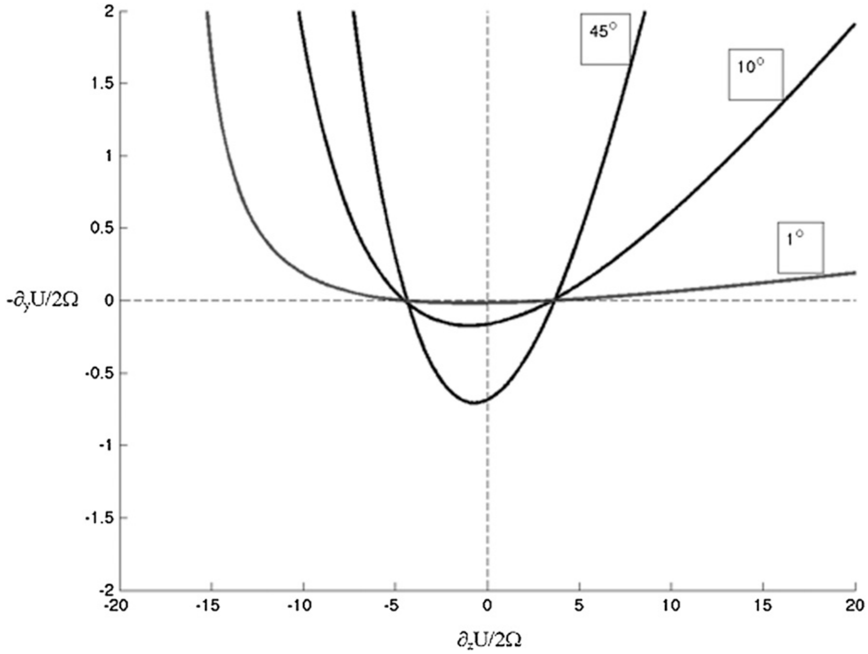

FIG. 4. The marginal curves for three latitudes for $2\Omega/N = 0.25$. Horizontal relative vorticity $(\partial U/\partial z)/2\Omega$ is along the horizontal axis of the figure (vertical relative vorticity $(\partial U/\partial y)/2\Omega$ is along the vertical axis). Negative vertical relative vorticity flows destabilize more easily as the latitude decreases because the critical value become very small. By contrast, the domain of stability of positive vertical relative vorticity expands at lower latitudes. As the equator is approached, a negative horizontal relative vorticity can still destabilize a positive vertical relative vorticity flow [if $\mathrm{Ro}_y < -(1 + \mu^{-2})$], whereas a positive horizontal relative vorticity cannot (the whole of the first quadrant above becomes stable).

$$\mathrm{Ro}_z \approx \mathrm{Ro}_y. \tag{19}$$

When recast in terms of horizontal and vertical shear, (19) becomes

$$-\frac{\partial U}{\partial y} \approx \tan\phi \frac{\partial U}{\partial z}. \tag{20}$$

If $\partial U/\partial z$ is fixed and the latitude ϕ goes to zero, then $\partial U/\partial y$ goes to zero and the domain of stability in Fig. 4 becomes asymptotic to the whole of the first quadrant. Therefore, a flow with positive vertical relative vorticity can remain stable at the equator for sufficiently high (positive) values of horizontal relative vorticity. This extension of stability agrees with inertial Rayleigh instability.

4. Dispersion relation and energetics

The dispersion relation (6) is first illustrated for rather strong stratification, strong vertical shear, and no horizontal shear in Fig. 5. The frequency being invariant to wavenumber changes $\mathbf{k}$ to $-\mathbf{k}$, so the locus of constant frequency in l–m space is symmetric with respect to the origin and only the half space ($m > 0$) is shown. Nearly horizontal wavenumbers (vertical wave crests) are stable with frequencies bounded by N. As the wavenumber orientation increases, the frequency decreases rapidly at first and vanishes for some critical nearly vertical orientation and a sector of instability opens. The maximum growth rate reaches 0.6, in units of 2Ω. The property that the frequency of internal waves does not depend on scale but only on orientation extends to the unstable wave: only particular wave crests angles are selected. Scales are arbitrary as long as they are small compared to the mean flow scales, the major working hypothesis here. The unstable sector is not symmetric with respect to the $l = 0$ axis but is centered around the direction of the mean buoyancy gradient. Unstable wave crests can show more or less tilt than the mean isopycnal surface indicating a variety of energy transfers. In the case shown here, the maximum growth rate is found for wave displacements nearly along the mean isopycnal surface.

When the frequency is real (and nonzero), the group velocity is normal to $\mathbf{k}$ and its value $(1/|k|)\partial_\theta \omega$ shows that it points downward everywhere for $m > 0$ (upward for $m < 0$). Right at the stability boundary the group velocity is not defined, but the largest group velocities are found

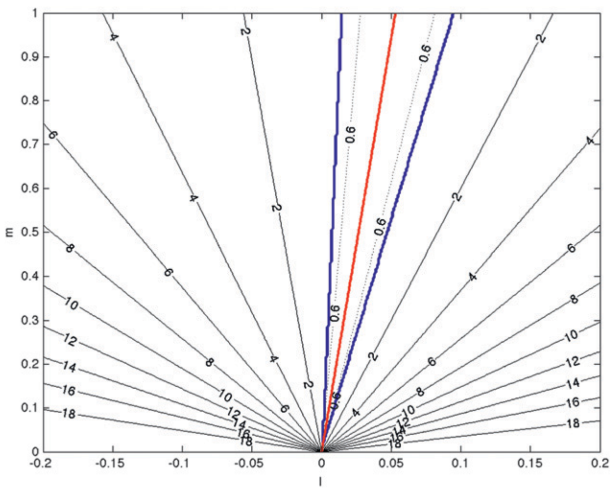

FIG. 5. Constant frequency locus in l–m space with real (imaginary) frequency drawn with solid (dotted) curves. The frequencies are nondimensionalized by 2Ω. The blue lines indicate zero frequency and form the boundary of the unstable sector. The red line marks the direction of ∇B. Parameters are $\phi = 45°$, $2\Omega/N = 0.05$, $\partial_z U/2\Omega = -30$, and $\mathrm{Ro}_z = 0$.

on the stable side of that boundary in Fig. 5. Neighboring stable waves can quickly send a signal (near horizontally here) of the existence of the nearby existence of an unstable region.

The consideration of energetics is essential to find the physical nature of the instability. To derive the energy equation, the momentum equations (2a)–(2e) are multiplied by **u** and averaged over a wavelength (an operation indicated by the brackets) to obtain

$$\partial_t \mathrm{KE} = -\langle uv\rangle \partial_y U - \langle uw\rangle \partial_z U + \langle bw\rangle, \qquad (21)$$

with $\mathrm{KE} = ½\langle |u|^2\rangle$ the perturbation kinetic energy per unit mass. Similarly, the buoyancy equation is multiplied by b and averaged to obtain

$$\partial_t \mathrm{PE} = -\langle bv\rangle \partial_y B/\partial_z B - \langle bw\rangle \qquad (22)$$

with the perturbation potential energy

$$\mathrm{PE} = \frac{1}{2}\langle b^2\rangle/\partial_z B.$$

Adding (21) and (22) gives the equation for the perturbation total energy $E = \mathrm{KE} + \mathrm{PE}$:

$$\partial_t E = -\langle uv\rangle \partial_y U - \langle uw\rangle \partial_z U - \langle bv\rangle \partial_y B/\partial_z B. \qquad (23)$$

Choose a real unstable wave of the form

$$\psi = (\psi_0 e^{i\theta} + \psi_0^* e^{-i\theta})e^{\omega_I t},$$

where $\theta = ly + mz$. Values of u, v, w, b, and the wave correlations that occur in (24) can be computed to be

$$\langle uv\rangle = m(mZ_{az} + lZ_{ay})A/\omega_I$$

$$\langle uw\rangle = l(mZ_{az} + lZ_{ay})A/\omega_I$$

$$\langle bw\rangle = l(m\partial_y B - l\partial_z B)A/\omega_I$$

$$\langle bv\rangle = -m(m\partial_y B - l\partial_z B)A/\omega_I$$

$$\mathrm{KE} = \frac{1}{2}\left(m^2 + l^2 + \frac{(mZ_{az} + lZ_{ay})^2}{\omega_I^2}\right)A$$

$$\mathrm{PE} = \frac{(m\partial_y B - l\partial_z B)^2}{\partial_z B}A/2\omega_I^2$$

in which $A = 2|\psi_0|^2 e^{2\omega_I t}$. To identify the various energy contributions to the growth rates ω_I, it is best to divide the various terms in (23) by the total energy E since the sum of the various energy fluxes on the right-hand side becomes simply $2\omega_I$. The results are shown in Fig. 6 for the parameters of the previous case. If $\theta_{\max}$ is the wavenumber orientation of the maximum growth rate, PE dominates for $\theta > \theta_{\max}$ and KE dominates for $\theta \le \theta_{\max}$. Furthermore, the term involving the buoyancy flux $\langle bv\rangle$ dominates the energetics for $\theta > \theta_{\max}$ and the term involving the $\langle uw\rangle$ Reynolds stress dominates for $\theta \le \theta_{\max}$. For $\theta > \theta_{\max}$, the wave displacements occur at an angle less than the mean isopycnal and conversion of mean potential energy is possible. For $\theta \le \theta_{\max}$, the mean kinetic energy source associated with the mean vertical shear becomes the primary energy flux. In the instability sector of Fig. 5, the wavenumber directions to the left of ∇B are caused by a transfer of mean potential energy, whereas those to the right are caused by a transfer of mean kinetic energy. When negative (positive) vertical relative vorticity is added, a positive (negative) contribution of mean kinetic energy fluxes also occurs in agreement with inertial instability. If the focus is on the maximum growth rate, the dominant contributor is the mean kinetic energy transfer. It occurs for a direction close to ∇B, justifying the hypothesis of symmetric instability that assumes fluid motions along isopycnal surfaces. However, as the stratification weakens (with larger μ), the energy transfer to the unstable wave becomes more equipartitioned between mean kinetic and mean potential energy fluxes.

As a second example, consider the instability that occurs at low latitudes for lower stratification, strong negative horizontal relative vorticity, and no vertical relative vorticity in Fig. 7a. The unstable sector is now very large. The growth rates are strong ~4 (in 2Ω unit) and the maximum now occurs for nearly horizontal wavenumbers

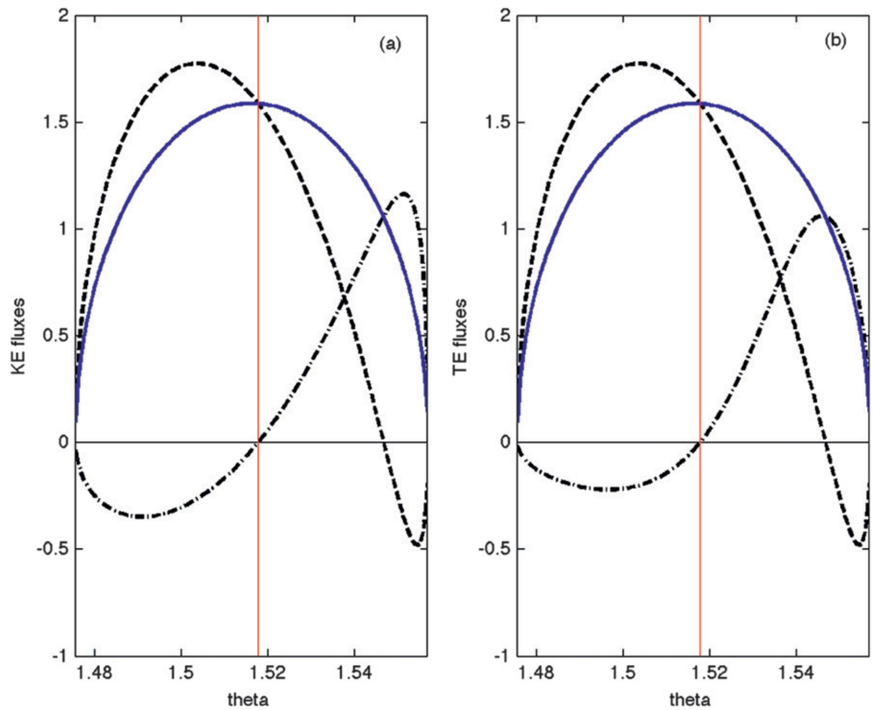

FIG. 6. Energy fluxes as function of the wavenumber vector orientation θ for parameters of Fig. 5. The thin red line marks the direction of ∇B. (a) Kinetic energy fluxes: $-\langle uw\rangle\partial_z U$ (dashed), $\langle bw\rangle$ (dashed–dotted), and total (blue). (b) Total energy fluxes: $-\langle uw\rangle\partial_z U$ (dashed), $-\langle bv\rangle\partial_y B/\partial_z B$ (dashed–dotted), and total (blue).

(or vertical wave crests). The source of instability comes entirely from the mean kinetic energy (not shown). Just changing the sign to positive Ro_y in Fig. 7b shows profound modifications: the unstable sector is much reduced and the growth rates are a factor of 10 weaker than in the previous case. Note that, in contrast to the two previous cases, the direction of ∇B is now within the stable sector. The unstable waves have displacements directions that are always less inclined than the mean isopycnal surfaces and the mean potential energy flux is positive. Both mean kinetic and mean potential energy fluxes contribute to the instability.

5. Growth rates

Of course, only the growth rates allow judgment of the strength of the instability and of its geophysical importance. Maximum growth rates are easily obtained from (10). They vary with the three adimensional numbers Ro_z, Ro_y, and the stratification parameter μ, all of which depending on latitude. These dependencies are shown in a series of maps with the maximum growth rates given in 2Ω units.

a. *Variation with horizontal relative vorticity* Ro_y

The Rossby number Ro_y (a measure of horizontal relative vorticity) is the major parameter allowing the results of this paper to be discussed. Figure 8a shows the increase of the growth rate with $|\mathrm{Ro}_y|$ at midlatitude (45°) for several values of $2\Omega/N$. Even though the vertical relative vorticity vanishes ($\mathrm{Ro}_z = 0$), large enough values of $|\mathrm{Ro}_y|$ allow the instability. The threshold values of Ro_y are large when stratification dominates rotation and the growth rates are less than $O(1)$. As the stratification decreases, however, the instability becomes very efficient—both in terms of the value of the growth rates (an order of magnitude stronger) and of the reduction of the stability interval along Ro_y. For the same parameter values but at equatorial latitudes (5°), Fig. 8b shows a dramatic change. The growth rates are now much smaller than in Fig. 8a except for negative Ro_y and reduced stratification ($2\Omega/N = 0.25$)—an indication of a powerful instability favoring negative horizontal relative vorticity.

b. *Variation with vertical relative vorticity* Ro_z

The influence of vertical relative vorticity on the previous picture is illustrated by showing maps of the growth rates in Ro_y–Ro_z space, Figs. 9a and 9b giving the growth rates at midlatitude (45°) and equatorial latitude (5°), respectively, for a case of strong stratification $2\Omega/N = 0.05$. Figure 9a strengthens quantitatively what has been said before about the instability favoring strong negative

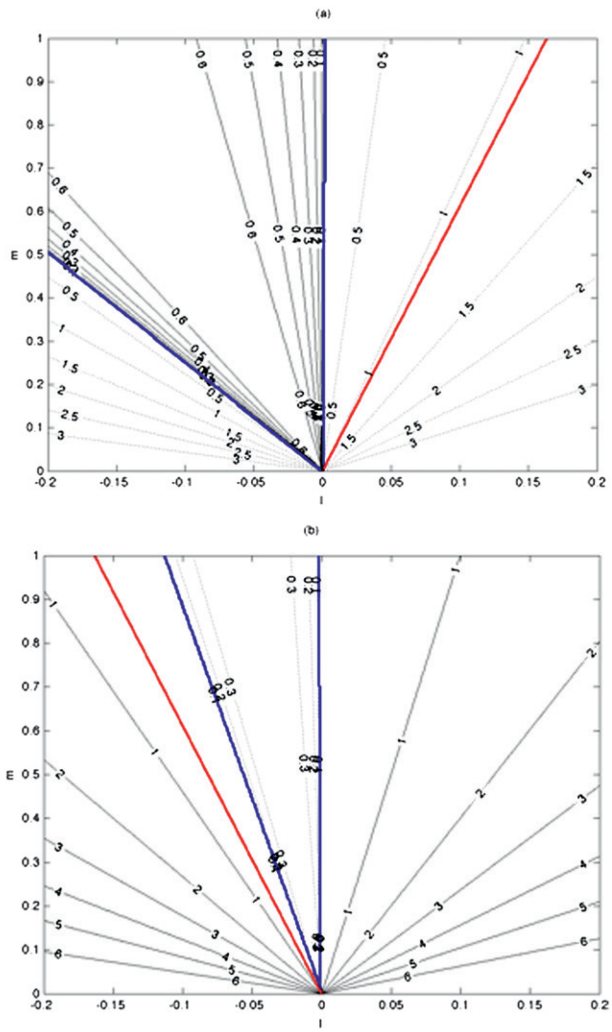

FIG. 7. Constant frequency locus in l–m space: real (imaginary) frequency shown by solid (dotted) curves. The frequencies are adimensionalized by 2Ω. The blue lines indicate zero frequency and form the boundary of the unstable sector. The red line marks the direction of ∇B. (a) Parameters are $\phi = 5°$, $2\Omega/N = 0.05$, $\partial_z U/2\Omega = -30$, and $Ro_z = 0$. (b) Parameters as in (a), but $\partial_z U/2\Omega = +30$.

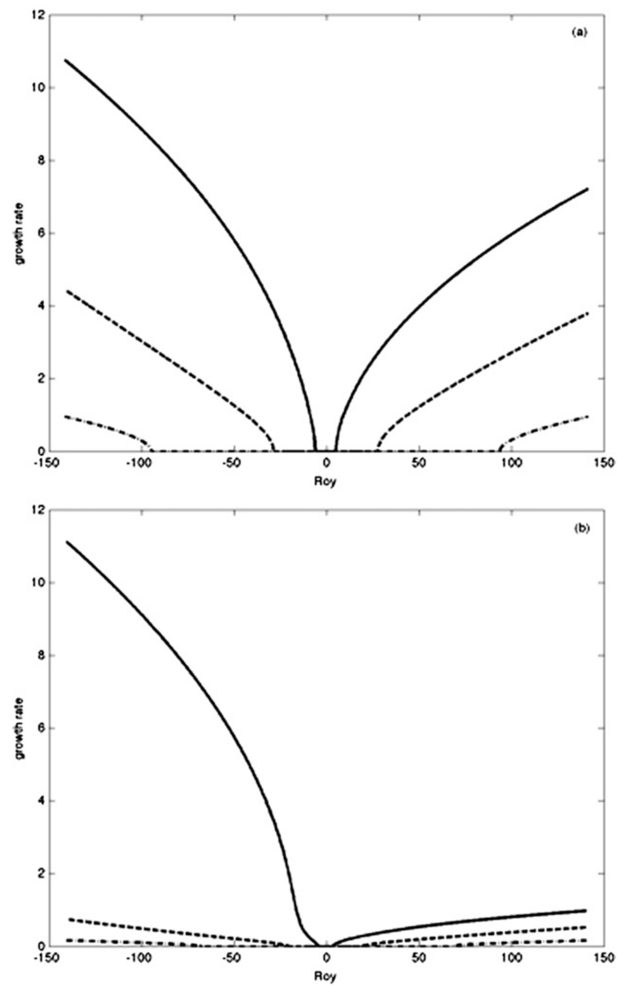

FIG. 8. Growth rates (in 2Ω units) against Ro_y (horizontal relative vorticity) for $Ro_z = 0$ (no vertical relative vorticity) and $2\Omega/N = 0.015$ (dashed–dotted), $2\Omega/N = 0.05$ (dashed), and $2\Omega/N = 0.25$ (solid). Latitudes are (a) $\phi = 45°$ and (b) $\phi = 5°$. As the stratification decreases, the instability interval and the growth rates increases. At midlatitudes in (a), the growth rates depend weakly on the sign of Ro_y as the diagram is nearly symmetric. At low latitudes and low stratification, a major asymmetry appears with negative horizontal relative vorticity generating the largest growth rates.

vertical relative vorticity. Unstable jets with positive vertical relative vorticity need to be associated with very large values of horizontal relative vorticity Ro_y to exhibit positive growth rates as well. The growth rate decreases markedly at low latitudes but, of course, the critical value of the required horizontal shear becomes also rather small with f. For weaker stratification $2\Omega/N = 0.25$ and at midlatitudes, jets with positive vertical relative vorticity can exhibit large growth rates for Ro_y values as small as $O(5)$ in Fig. 10a. The asymmetry between positive and negative values of Ro_y is still rather modest, but it dominates the low-latitude picture in Fig. 10b. The growth rates are small for positive Ro_y to become an order of magnitude larger for negative Ro_y. The condition (19) or $Ro_y = -(1 + \mu^{-2})$ becomes relevant to rationalize the presence of these very strong growth rates. Note that the influence of the value of the vertical relative vorticity (Ro_z) becomes negligible in this region of parameter space.

c. *Variations with latitude*

Of course, for applications to the ocean or atmosphere, it is important to find out for which values of shears and stratification the zonal jets can become unstable, as the results are strongly latitude dependent. The variation of the growth rates with latitude is shown in a series of maps in Figs. 11 and 12. Figure 11 show the variations in

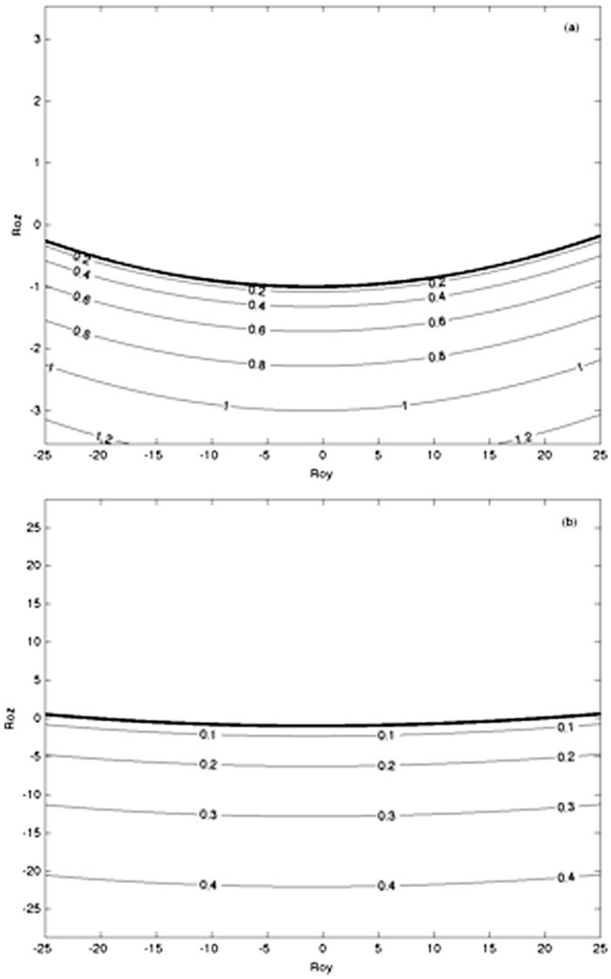

FIG. 9. Growth rates (in 2Ω units) for a strong stratification $2\Omega/N = 0.05$ in Ro_z–Ro_y space (a) at latitude $\phi = 45°$ with contour interval = 0.2 and (b) at latitude $\phi = 5°$ with contour interval = 0.1. The bold curve is the marginal (zero frequency) stability condition (12). The classical inertial stability limit of vanishing vertical absolute vorticity component or $\mathrm{Ro}_z = -1$ dominates the picture. This implies strong negative vertical relative vorticity for instability at midlatitudes in (a). At low latitudes in (b), the flow can now be unstable for very small negative vertical relative vorticity as f is small, but note the association with smaller growth rates.

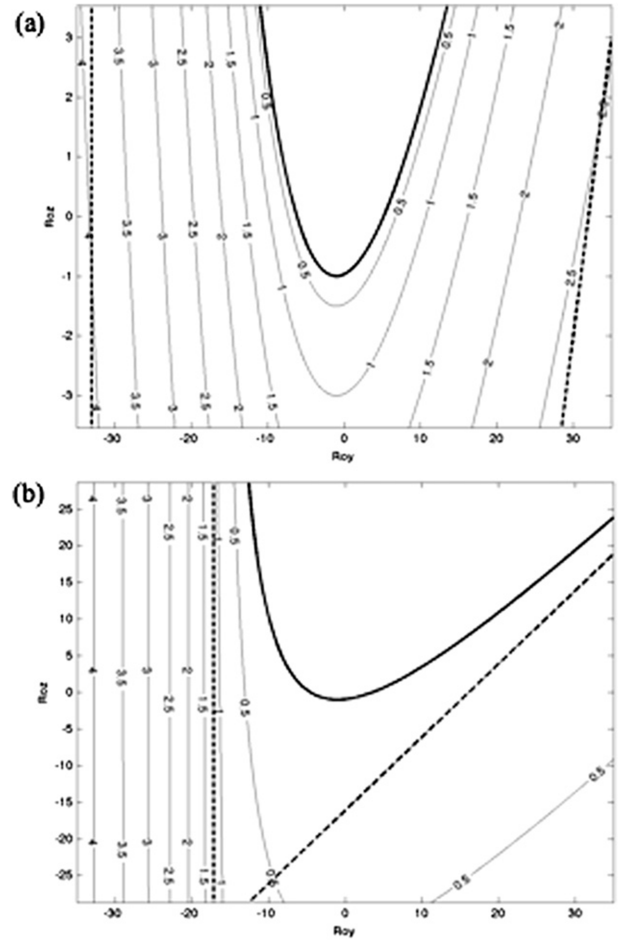

FIG. 10. Growth rates (in 2Ω units) for a weak stratification $2\Omega/N = 0.25$ in Ro_z–Ro_y space (a) at latitude $\phi = 45°$ with contour interval = 0.5 and (b) at latitude $\phi = 5°$ with same contour interval. The bold curve is the marginal (zero frequency) stability condition (12). The vertical asymptote (dashed) obeys $\mathrm{Ro}_y = -(1 + \mu^{-2})$, condition (19). The oblique asymptote (dashed) obeys $\mathrm{Ro}_z = \mathrm{Ro}_y - \mu^{-2}$. For large μ, the former is inertial instability, with the meridional absolute vorticity component vanishing for $\mathrm{Ro}_y = -1$. At the difference of Fig. 9, the dependence on horizontal relative vorticity through Ro_y enters the picture. For sufficiently large values, positive vertical relative vorticity flows become unstable as well. At low latitude in (b), the strong asymmetry with respect to the sign of Ro_y appears, with the instability favoring negative Ro_y as the vertical asymptote is approached. The domain of stability is larger and the growth rates are smaller for positive Ro_y.

latitude–horizontal relative vorticity $(\partial U/\partial z)/2\Omega$ parameter space for strong stratification with negative vertical relative vorticity $(-\partial U/\partial y)/2\Omega = -0.25$ kept constant. For strong stratification, the growth rates decrease as the latitude decreases, but at the same time the stability boundaries merge at low latitudes and the flow is then always unstable for latitudes less than 15°. These are symptoms of the effect of the vertical component of absolute vorticity. For weaker stratification, the growth rates become much stronger than previously and the asymmetry between positive and negative Ro_y stands out at low latitudes. Only the presence of the horizontal component of the earth's vorticity and the control by the horizontal component of the absolute vorticity can explain this effect.

Finally, the combined effect of stratification and latitude is shown in Fig. 12 for two values of horizontal relative vorticity $(\partial U/\partial z)/2\Omega = +15$ and -15 and constant vertical relative vorticity as previously. When the horizontal relative vorticity is positive (Fig. 12a), growth rates increase as stratification weakens but saturate for

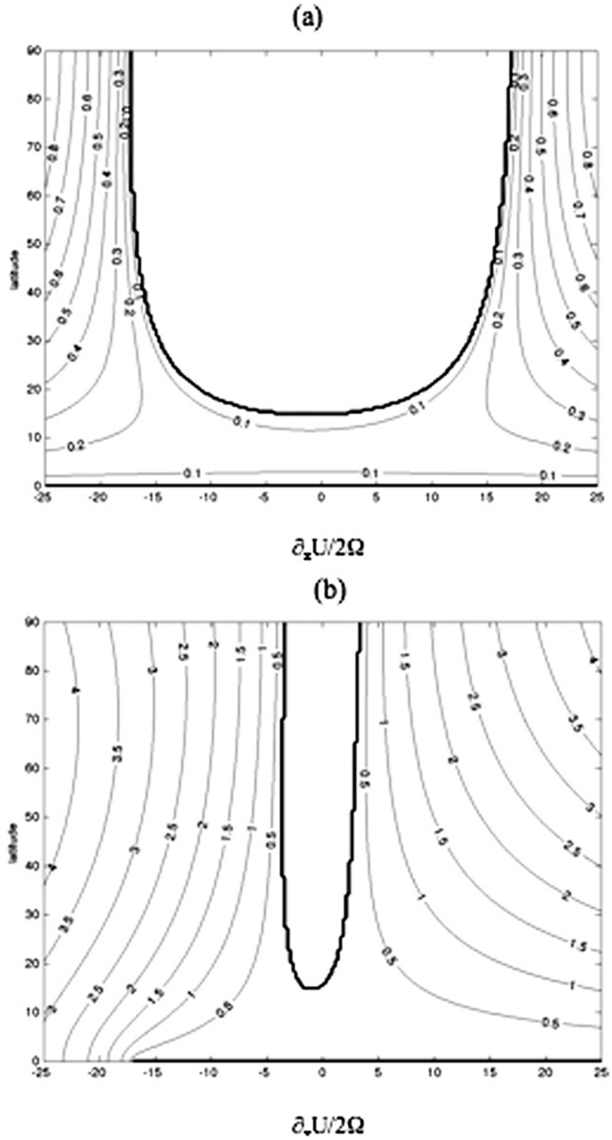

FIG. 11. Growth rates (in 2Ω units) as a function of latitude and horizontal relative vorticity $(\partial U/\partial z)/2\Omega$ for constant negative vertical relative vorticity $(-\partial U/\partial y)/2\Omega = -0.25$. The bold curve is the marginal stability condition (12). (a) Strong stratification $2\Omega/\mathrm{N} = 0.05$. (b) Weak stratification $2\Omega/\mathrm{N} = 0.25$. The red curve is condition (19). As the stratification weakens in (b), the domain of stability is reduced strongly and the growth rates increase by a factor of 4. The strong asymmetry with respect to the sign of vertical shear stands out at low latitude in (b) with far larger growth rates for negative horizontal relative vorticity.

$2\Omega/N$ beyond about 0.5. The effect is strong at midlatitudes but negligible at low latitudes (growth rates remain small whatever the stratification). Hence, although the instability occurs for all vertical shears for latitudes less than 15°, the instability is weak. Instead, if the vertical shear is negative, the situation is very different and weak stratification indeed boost growth rates at low latitudes (Fig. 12b). Condition (18) can be expressed in terms of vertical shear and latitude as $2\Omega/N \approx [-\cos\phi^2(\mathrm{Ro}_y + 1)]^{-1/2}$, so that stratification increases when $|\mathrm{Ro}_y|$ increases. For realistic values of horizontal relative vorticity $(\partial U/\partial z)/2\Omega = -15$, corresponding values of $2\Omega/N$ are about 0.25 at low latitudes, so the stratification does not have to be weak compared to rotation to show this new asymmetry between negative and positive vertical shears.

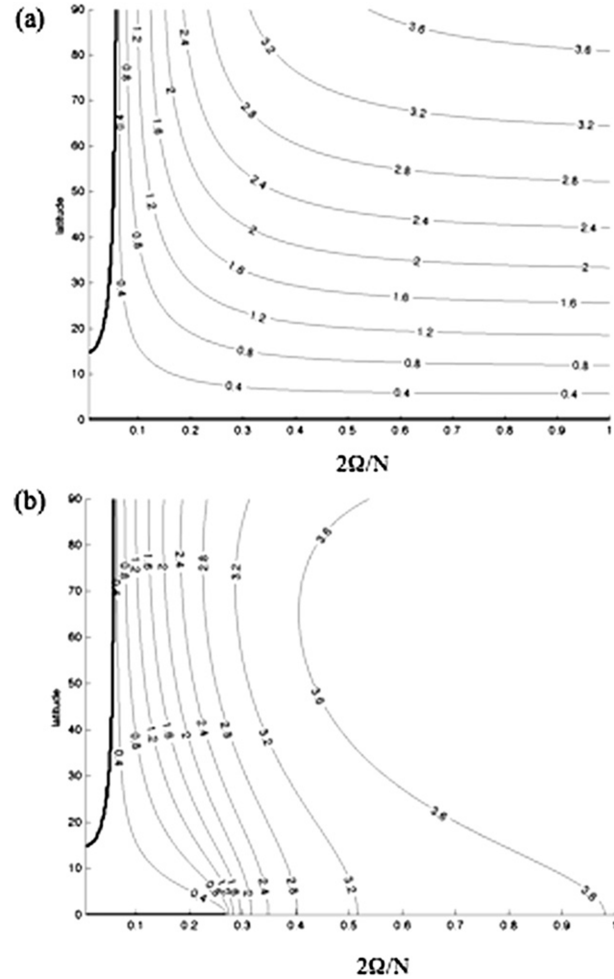

FIG. 12. Growth rates (in 2Ω units) as a function of latitude and parameter $2\Omega/\mathrm{N}$. The negative vertical relative vorticity is constant, $(-\partial U/\partial y)/2\Omega = -0.25$. The black bold curve is the marginal stability condition (12). (a) Positive horizontal relative vorticity $(\partial U/\partial z)/2\Omega = +15$. (b) Negative horizontal relative vorticity $(\partial U/\partial z)/2\Omega = -15$. In both cases, the growth rates increase as the stratification weakens until $2\Omega/\mathrm{N} \approx 0.5$, at which value they saturate. The growth rates also decrease with latitude. For latitudes less than 15°, (a) they remain small for positive horizontal relative vorticity but (b) increase rapidly to $O(1)$ for values of $2\Omega/\mathrm{N} \approx 0.25$ for negative values.

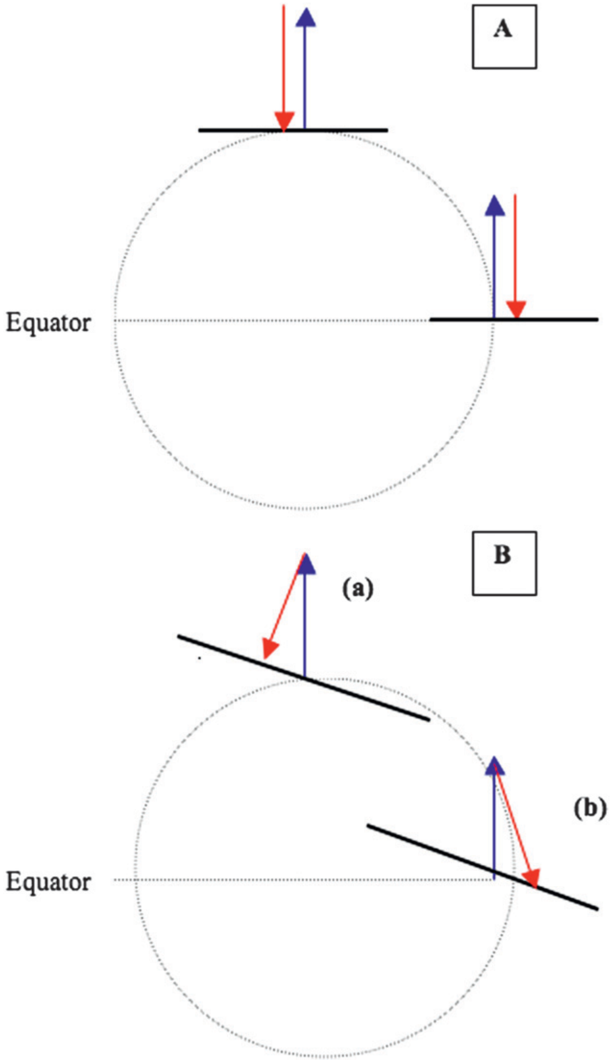

FIG. 13. Several situations of marginal stability are pictured. The earth's vorticity vector $2\boldsymbol{\Omega}$ is in blue, and the relative vorticity vector $\mathbf{Z}_r$ is in red. The thick black lines are the isopycnal surfaces (B = cst). The marginal stability condition (Ertel PV = 0) requires by construction that the absolute vorticity vector $\mathbf{Z}_a = \mathbf{Z}_r + 2\boldsymbol{\Omega}$ is parallel to the B surface and the thermal wind balance allows in turn to find the direction of $\mathbf{Z}_a$ along that surface. Case A: Suppose that the B surfaces are normal to the earth's rotation vector $\boldsymbol{\Omega}$. They are horizontal at the pole and this requires a very strong stratification (large N^2). The marginal condition is just that the vertical absolute relative vorticity vanishes, $Z_{rz} = -2\Omega_z$. This is inertial instability with the mean flow varying in y only and unstable motions in the horizontal x–y plane. By translation of the figure from the pole to the equator, the same inertial instability now occurs when the meridional component of absolute vorticity vanishes, $Z_{ry} = -2\Omega_y$. But, the B surfaces are now vertical (small N^2). The unstable motions are in the vertical x–z plane. Case B: Consider now the case when the B surfaces are not perpendicular to $2\boldsymbol{\Omega}$. In (a) at high latitudes, the B surfaces slope up toward the pole and the vertical shear of the mean flow is positive. Marginal stability is reached with positive horizontal and vertical components of absolute vorticity. By translation to a low latitude in (b), the B surfaces now shoal toward the equator and the mean vertical shear becomes negative. Marginal stability is reached with negative horizontal and positive vertical components of absolute vorticity. A powerful instability develops when the flow becomes supercritical.

6. Summary and discussion

The following summary can be read with the help of a visualization of the marginal condition of instability on the sphere in Fig. 13 (with its own commentary). Rayleigh (1917) discovered that inertial instability occurs for a homogeneous fluid when circulation decreases with distance from the rotation axis. However, the ocean and atmosphere are stratified and geostrophically balanced mean flows are associated with a tilt of the isopycnal (or potential temperature) surfaces. Symmetric instability has focused in the past on the case of stratification dominating over rotation (Hoskins 1974). For strong stratification (large Richardson number), the perturbed motions remain quasi horizontal and vertical absolute vorticity $Z_{az} = f - \partial U/\partial y$ has to be negative for the flow to be unstable recovering Rayleigh's result. However, even in the absence of vertical relative vorticity (no horizontal shear), an instability is still possible provided enough horizontal relative vorticity is present (the Richardson number Ri has to be less than 1). With a geostrophic mean flow, the marginality condition Ri = 1 can be rewritten as a Burger number condition $(f^{-1}Ns)^2 = 1$ in which s is the slope of the mean isopycnal surfaces. Hence, an $O(1)$ Burger number is the expected end result of the life cycle of short-scale unstable perturbations working their way to restore stability of the mean flows. This is a complement (rather than an alternative) to the classical explanation of an $O(1)$ Burger number through the Rossby geostrophic adjustment process based on internal waves radiation. When vertical relative vorticity is included, the asymmetry of positive and negative vertical relative vorticity (horizontal shear) of the mean flow becomes the structuring element of symmetric instability. This asymmetry is found to be very sensitive to the rotation/stratification ratio. Weakening the stratification reduces the values of critical shears, and positive vertical relative vorticity flows can be destabilized for realistic values of horizontal relative vorticities.

If the stratification is too weak however, the traditional approximation becomes unacceptable. The parameter coverage of the unstable regimes of short internal waves on shear flows has been extended here to include this full representation of the Coriolis terms. Giving up the traditional approximation, a new asymmetry emerges but this time between positive and negative horizontal components of relative vorticity (vertical shear) of the mean flow. The doorway to this regime occurs from condition (19), $\tilde{f}Z_{ay} + N^2 \approx 0$, which can be expressed as $N^{-1}2\Omega \approx [-\cos^2\phi(\mathrm{Ro}_y + 1)]^{-1/2}$ or $\mathrm{Ro}_y \approx -(1 + \mu^{-2})$, or still $\mathrm{Ri}^{1/2} \approx -\mu/(1 + \mu^2)$. The instability condition obviously requires that the horizontal vertical vorticity has to be negative ($\mathrm{Ro}_y < -1$) and is favored by weak stratification ($\mu = 2\Omega \cos\phi/N \gg 1$). If N vanishes, it reduces to the Rayleigh type inertial instability condition with the vanishing of the horizontal component of absolute vorticity

$$Z_{ay} = \tilde{f} + \frac{\partial U}{\partial z} = 0.$$

The zonal and vertical mean momentum equations are coupled by the Coriolis force due to the meridional component of the earth's rotation, and unstable perturbations have nearly vertical orientations. The important point here is that the stratification does not have to be that weak to show these new effects. Indeed, values of $2\Omega/N$ as small as 0.25 are found for critical vertical shears $O(10^{-3}\ \mathrm{s}^{-1})$. The geographic position in latitude has a strong influence on the regimes of stability. For strong stratification, the domain of instability increases with lower latitudes but the growth rates decrease as f decreases. This is the influence of the vertical component of the earth's rotation. For weak stratification, the influence of the meridional component of the earth's rotation shows up through the asymmetry amplifying the growth rates of negative horizontal relative vorticity flows over positive ones; that is, the instability favors the situation when the mean isopycnal surfaces shoal toward the equator. This new asymmetry is enhanced at low latitudes essentially because the other traditional symmetric instability due to the vertical component of the earth's rotation becomes ineffective.

There is usually a wide sector of internal wave orientations that allow instability for a given mean flow. When the waves slope at an angle larger than the mean isopycnal surfaces, the Reynolds stresses of the waves dominate and the energy source is the mean kinetic energy. If the angle is smaller, the buoyancy fluxes dominate and the energy source is the available potential energy. Both sources are important even though the maximum growth rates are usually dominated by the mean kinetic energy fluxes. Whether such instabilities are important contributors to the necessity of diapycnal mixing in the ocean is unknown. Note that the theory predicts wave orientations only and that spatial scales are arbitrary at this point, so the existence of a direct cascade to dissipative scales is unknown.

The association of low stratification values and large vertical shear are readily found in oceanic mixed layers or near western boundary currents. Strong vertical shears have also been observed for the equatorial deep jets in the Pacific and Atlantic (Firing 1987; Gouriou et al. 2001), and the observations point to increased mixing of tracers in westward jets. Ménesguen et al. (2009) have proposed inertial instability processes (under the traditional approximation) to rationalize these observations. Whether the stronger instability found here for negative horizontal relative vorticity is at work to control the jets remains to be assessed.

In the atmospheric case, symmetric instabilities have been found important for the explanation of frontal rainbands (Bennett and Hoskins 1979; Seltzer et al. 1985) within the context of the traditional approximation. There is also a debate on mesoscale atmospheric dynamics about the identification of the lift responsible for the precipitation (Schultz et al. 2000), and the instability explored here for low rotation/stratification ratios could well play a role once ordinary gravitational convection has preconditioned a state of weak stratification. At low latitudes, consideration of the meridional component of the earth's rotation favors the instability of negative horizontal relative vorticity, that is, easterlies with wind increasing upward. Whether this instability plays a role in the initiation of mesoscale features in tropical cyclones could provide test elements of the theory.

Finally, the existence of instabilities of internal waves in geostrophically balanced flows is interesting from another point of view. Most of what we know about the large-scale circulation in the ocean–atmosphere system is based on a frequency separation between the geostrophic balanced motions and the internal gravity wave band. But, here internal gravity waves of zero (real) frequency explode spontaneously from a balanced state. The examples developed here give support to the fallacy of the high–low frequency separation, which have been outlined by McWilliams et al. (2004), Vanneste and Yavneh (2004), and Molemaker et al. (2005) in several contexts under the traditional approximation. The role for ocean energetics of such "loss of balance effects" between the mesoscale and the gravity waves are virtually unknown (Wunsch and Ferrari 2004). As stressed by Molemaker et al. (2005), they may be important for identification of the paths to dissipation in the ocean.

Acknowledgments. ACdV thanks the reviewers and one especially for their many suggestions for improvements as well as Claire Ménesguen for her useful comments on a first draft of this paper.

REFERENCES

Bennett, D. A., and B. J. Hoskins, 1979: Conditional symmetric instability—A possible explanation for frontal rainbands. *Quart. J. Roy. Meteor. Soc.,* **105,** 945–962.

Bluestein, H. B., 1993: *Observations and Theory of Weather Systems.* Vol. II, *Synoptic-Dynamic Meteorology in Midlatitudes,* Oxford University Press, 594 pp.

Booker, J. R., and F. P. Bretherton, 1967: The critical layer for internal gravity waves in a shear flow. *J. Fluid Mech.,* **27,** 513–539.

Charney, J. G., 1947: The dynamics of long waves in a baroclinic westerly current. *J. Meteor.,* **4,** 135–163.

——, 1973: Lecture notes on planetary fluid dynamics. *Dynamic Meteorology,* P. Morel, Ed., Riedel, 99–351.

Colin de Verdière, A., and R. Schopp, 1994: Flows in a rotating spherical shell: The equatorial case. *J. Fluid Mech.,* **276,** 233–260.

Drazin, P. G., and W. H. Reid, 1981: *Hydrodynamic Instability*. Cambridge University Press, 527 pp.

Eady, E. T., 1949: Long waves and cyclone waves. *Tellus,* **1,** 33–52.

Emmanuel, K. A., 1994: *Atmospheric Convection*. Oxford University Press, 580 pp.

Firing, E., 1987: Deep zonal currents in the central equatorial Pacific. *J. Mar. Res.,* **45,** 791–812.

Gerkema, T., J. T. F. Zimmerman, L. R. M. Maas and H. van Haren, 2008: Geophysical and astrophysical fluid dynamics beyond the traditional approximation. *Rev. Geophys.,* **46,** RG2004, doi:10.1029/2006RG000220.

Gouriou, Y. C., and Coauthors, 2001: Deep circulation in the equatorial Atlantic Ocean. *Geophys. Res. Lett.,* **28,** 819–822.

Grimshaw, R., 1975: Internal gravity waves: Critical layer absorption in a rotating fluid. *J. Fluid Mech.,* **70,** 287–304.

Haine, T. W. N., and J. Marshall, 1998: Gravitational, symmetric, and baroclinic instability of the ocean mixed layer. *J. Phys. Oceanogr.,* **28,** 634–658.

Hoskins, B. J., 1974: The role of potential vorticity in symmetric stability and instability. *Quart. J. Roy. Meteor. Soc.,* **100,** 480–482.

Hua, B. L., D. W. Moore, and S. Le Gentil, 1997: Inertial nonlinear equilibration of equatorial flows. *J. Fluid Mech.,* **331,** 345–371.

Jeffery, N., and B. Wingate, 2009: The effect of tilted rotation on shear instabilities at low stratification. *J. Phys. Oceanogr.,* **39,** 3147–3161.

Jones, W. L., 1967: Propagation of internal gravity waves in fluids with shear flow and rotation. *J. Fluid Mech.,* **30,** 439–448.

Joyce, T. M., L. N. Thomas, F. Bahr, 2009: Wintertime observations of Subtropical Mode Water formation within the Gulf Stream. *Geophys. Res. Lett.,* **36,** L02607, doi:10.1029/2008GL035918.

Lindzen, R. S., 1988: Instability of plane parallel shear flow (towards a mechanistic picture of how it works). *Pure Appl. Geophys.,* **126,** 103–121.

McWilliams, J. C., M. J. Molemaker, and I. Yavneh, 2004: Ageostrophic, anticyclonic instability of a geostrophic, barotropic boundary current. *Phys. Fluids,* **16,** 3720–3725.

Ménesguen, C., B. L. Hua, M. D. Fruman, and R. Schopp, 2009: Intermittent layering in the Atlantic equatorial deep jets. *J. Mar. Res.,* **67,** 347–360.

Molemaker, M. J., J. C. McWilliams, and I. Yavneh, 2005: Baroclinic instability and loss of balance. *J. Phys. Oceanogr.,* **35,** 1505–1517.

Mooers, C. N. K., 1975: Several effects of baroclinic currents on the cross stream propagation of internal waves. *Geophys. Fluid Dyn.,* **6,** 245–275.

Ooyama, K., 1966: On the stability of baroclinic circular vortex: a sufficient criterion for instability. *J. Atmos. Sci.,* **23,** 43–53.

Rayleigh, L., 1917: On the dynamics of revolving fluids. *Proc. Roy. Soc. London,* **93A,** 148–154.

Schultz, D. M., P. N. Schumacher, and C. A. Doswell III, 2000: The intricacies of instabilities. *Mon. Wea. Rev.,* **128,** 4143–4148.

Seltzer, M. A., R. E. Passarelli, and K. A. Emmanuel, 1985: The possible role of symmetric instability in the formation of precipitation bands. *J. Atmos. Sci.,* **42,** 2207–2219.

Sheremet, V. A., 2004: Laboratory experiments with tilted convective plumes on a centrifuge: A finite angle between the buoyancy force and the axis of rotation. *J. Fluid Mech.,* **506,** 217–244.

Stone, P. H., 1966: On non geostrophic baroclinic stability. *J. Atmos. Sci.,* **23,** 390–400.

Straneo, F., M. Kawase, and S. C. Riser, 2002: Idealized models of slantwise convection in a baroclinic flow. *J. Phys. Oceanogr.,* **32,** 558–572.

Sun, W. Y., 1995: Unsymmetrical symmetric instability. *Quart. J. Roy. Meteor. Soc.,* **121,** 419–431.

Taylor, J. R., and R. Ferrari, 2010: Buoyancy and wind-driven convection at mixed layer density fronts. *J. Phys. Oceanogr.,* **40,** 1222–1242.

Vanneste, J., and I. Yavneh, 2004: Exponentially small inertia–gravity waves and the breakdown of quasigeostrophic balance. *J. Atmos. Sci.,* **61,** 211–223.

Wirth, A., and B. Barnier, 2008: Mean circulation and structures of tilted ocean deep convection. *J. Phys. Oceanogr.,* **38,** 803–816.

Wunsch, C., and R. Ferrari, 2004: Vertical mixing, energy, and the general circulation of the ocean. *Annu. Rev. Fluid Mech.,* **36,** 281–314.

Xu, Q., and J. H. E. Clark, 1985: The nature of symmetric instability and its similarity to convective and inertial instability. *J. Atmos. Sci.,* **42,** 2880–2883.